Networks of Injectable Microdevices Powered and Digitally Linked by Volume Conduction for Neuroprosthetics: a Proof-of-Concept

Laura Becerra-Fajardo
Department of Information and Communications Technologies
Universitat Pompeu Fabra
Barcelona, Spain
laura.becerra@upf.edu

Jesus Minguillon
Department of Signal Theory, Telematics and Communications
University of Granada
Granada, Spain
minguillon@ugr.es

Albert Comerma
Department of Information and Communications Technologies
Universitat Pompeu Fabra
Barcelona, Spain
albert.comerma@upf.edu

Antoni Ivorra
Serra Húnter Programme
Department of Information and Communications Technologies
Universitat Pompeu Fabra
Barcelona, Spain
antoni.ivorra@upf.edu

***Abstract*— Wireless power transfer (WPT) methods such as inductive coupling and ultrasounds are used as an alternative to electrochemical batteries to energize active implantable medical devices. However, existing WPT methods require the use of bulky components (e.g., coils) that hinder miniaturization. To avoid this, we proposed the use of volume conduction of high frequency (HF) current bursts to power and bidirectionally communicate with threadlike implants that can be used for electrical stimulation and sensing (e.g., electromyography acquisition). Here, we *in vitro* demonstrate that several wireless devices can be powered and digitally linked by volume conduction. Eleven devices were randomly placed in a saline medium and were enclosed by two electrodes connected to an external system. The system interrogated the devices, and the waveforms obtained by the external system's demodulator were digitally processed to decode the information sent by the devices through the same HF current bursts. Data was successfully decoded from the devices, independently of the power that each single device obtained. The WPT efficiency of volume conduction boosts when a massive number of devices are powered with a single external system, creating a network of microdevices for neuroprosthetics. This will allow to accomplish closed-loop control for neural interphases using highly miniaturized injectable devices.**

Keywords—wireless power transfer, volume conduction, AIMDs, electrical stimulation, neuroprosthetics, closed-loop control

I. Introduction

Some neuroprosthetic systems require to implement closed-loop control for electrical stimulation using signals acquired from the patient. This could, for example, help detect user intention by means of electromyography (EMG), or be used in the treatment of tremor in essential tremor and Parkinson's disease [1]. Additionally, to accomplish a smooth control, it is proposed the use of networks of miniaturized implantable sensors and stimulators with high selectivity [2].

Wireless power transfer (WPT) methods are frequently used as an alternative to electrochemical batteries to energize electronic implants. However, methods based on inductive coupling or ultrasounds have obtained high miniaturization levels at the expense of link efficiency, penetration depth or functionality [3], [4]. In [5] we proposed a method to power and control injectable microstimulators by applying -through textile electrodes- high frequency (HF) current bursts that flow through the tissues by volume conduction. The currents are picked-up by the implant's electrodes (located at the ends of the elongated body) and are rectified for powering and bidirectional communications (Fig. 1). This method avoids the use of bulky components as coils and batteries and conceives the implants as threadlike devices to be deployed by injection.

When used to power a single implant, the WPT method based on volume conduction may be less energy efficient than other powering methods. However, if several devices are enclosed by a single pair of external electrodes, the WPT efficiency is boosted by a factor proportional to that of the number of wireless devices present. This massive coexistence of threadlike microdevices (e.g., sensors and stimulators) could offer high selectivity for closed-loop control of networked neural interphases.

We demonstrated that injectable prototypes with an overall diameter of 0.97 mm can be powered and addressed to perform electrical stimulation using this WPT method [6]. We also demonstrated with semi-implantable devices a digital bidirectional communication protocol with 13 different commands, and the possibility to use the devices for EMG

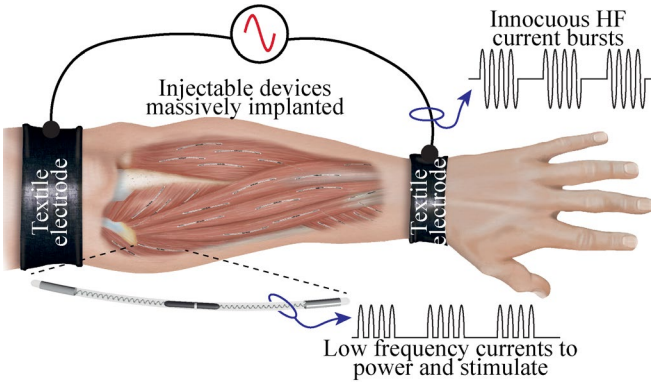

Fig. 1. Wireless power transfer method proposed for obtaining threadlike implants that can perform electrical stimulation and EMG sensing. The devices pick up the HF current bursts for powering and bidirectional communications. and rectify them for electrical stimulation.

sensing and electrical stimulation [7]. Yet the demonstrations performed are done with at most five wireless devices due to size limitations of the animal model (hindlimb of rabbit). Here we report the feasibility of powering and bidirectionally communicating with more than 10 microdevices using volume conduction, regardless of their position with respect to the external system's electrodes.

II. Methods

A. Electronic systems

The basic architecture of the external system has been described in [7]. It is composed of a HF generator and modulator (4064 by B&K Precision, Corp.) connected to a custom-made power amplifier consisting of fifteen high voltage amplification modules, based on a high speed, high voltage operational amplifier (ADA4870 by Analog Devices, Inc.), which are connected in series through transformers. The output of the power amplifier is connected in series to a sensing resistor for uplink demodulation, and to a pair of external electrodes. The modulating signal used to modulate the HF current bursts and the information for downlink is generated using a control unit commanded from a computer running Matlab (R2019b, by Mathworks, Inc). The sensing resistor for uplink is connected to a demodulation circuit that includes active band-pass filters.

The devices used here have the miniature electronic circuit described and demonstrated in [7] (Fig. 2a). The circuit has two dc-blocking capacitors to prevent dc currents, and a rectification subcircuit that provides a stable dc voltage for a low-power microcontroller (MKL03Z-32CAF4R by NXP Semiconductors N.V.), and the analog front-end for EMG acquisition. The circuit includes a demodulator for downlink communications, current limiters for electrical stimulation and a load modulation circuit for uplink communications. This circuit is connected to a pair of 30 AWG kynar wire electrodes (100-30R and 100-30TB by Multicomp Pro) that are held together using a 3D printed plastic structure that ensures that the electrodes are aligned and at a distance of 30 mm between center of electrodes (Fig. 2b). The structure includes a plastic holder to position the electrodes at specific locations with respect to the external electrodes.

To control several wireless devices using the same external system, a communication protocol was created to digitally control 256 wireless devices and groups of devices, and the possibility to configure the electrical stimulation and EMG acquisition parameters [7].

B. Test bench

The test bench used for this demonstration is based on the *in vitro* setup reported in [8]. Two 7 × 2.5 cm aluminum plates acting as external electrodes (1.2 mm thick, 1050A) and connected to the external system, were held parallel at 11 cm using two polycarbonate plates (Fig. 3a). A 1 × 1 cm grid made of cotton thread was sewed across the plates, 1.25 cm from the bottom of the structure. The structure was placed inside a 19 × 14 × 6.3 cm glass container filled up to 3 cm with saline with a conductivity similar to that of muscle tissue at 3 MHz (0.57 S/m) [9]. Multiple miniature electronic circuits were held in the border of the glass container, and the plastic structures holding the electrodes were immersed in the saline medium at different positions, as shown in Fig. 3b.

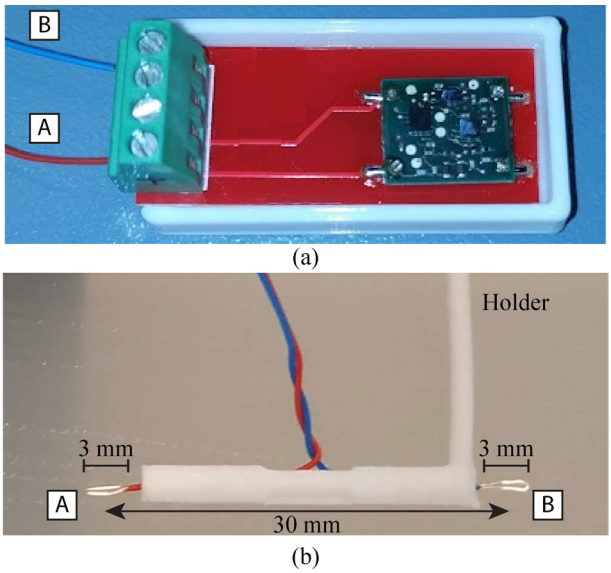

Fig. 2. Miniature electronic circuit (a) and electrodes (b) used for the demonstration. The plastic holder was used to locate the pair of electrodes in the saline test bench.

The HF current bursts applied by the external system were monitored using a differential active probe (TA043 by Pico Technology) and a current probe (TCP2020 by Tektronix, Inc.) connected to a battery-powered oscilloscope (TPS2014 by Tektronix, Inc.).

C. Digital processing and decoding algorithm

In [7] we reported a hardware-based decoding system for the external system. It included a comparator connected to the UART receiver of the control unit. Even though this approach has given very good results, it is susceptible to HF noise and to differences in the electric potential seen across the sensing resistor, which is proportional to the load modulation done by the wireless devices. For this reason, a different approach is proposed here, in which the hardware-based decoding is replaced by a digital processing and decoding approach. The battery powered oscilloscope was used to measure the output of the demodulation circuit of the external system (i.e., demodulator for uplink communications). The external system requested an uplink and then triggered the oscilloscope's acquisition.

The uplink waveforms obtained with the oscilloscope were analyzed offline using Matlab (R2019b, by Mathworks, Inc). The first step was to identify the time frame of interest: the time window when the data is expected to arrive to the external system. The algorithm identifies the saturation of the demodulator because of the HF bursts that are delivered by the external system when requesting an uplink. The start of the time frame of interest is defined 70 µs after this saturation. At this point, the wireless device delivers a flag, and immediately after, sends the information requested by the external system according to the communication protocol (e.g., when ping is requested, an 8-bit frame acknowledge (ACK) is transmitted by the device).

The second step was to identify the peaks during this time frame. As the bidirectional communication is done at 256 kbps,

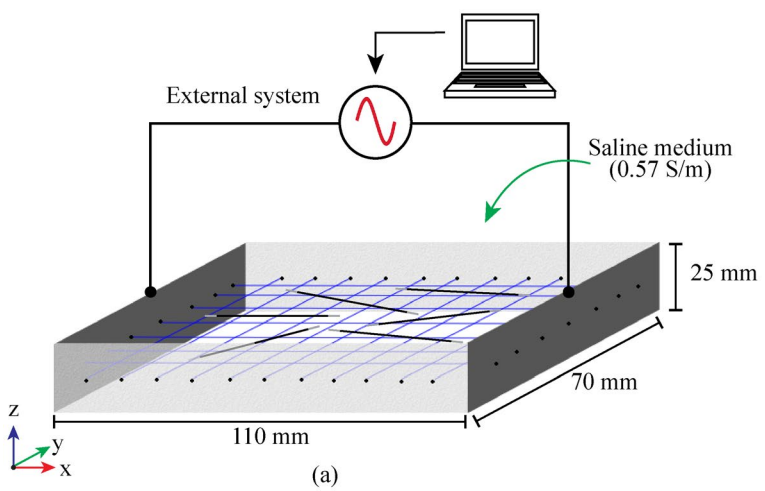

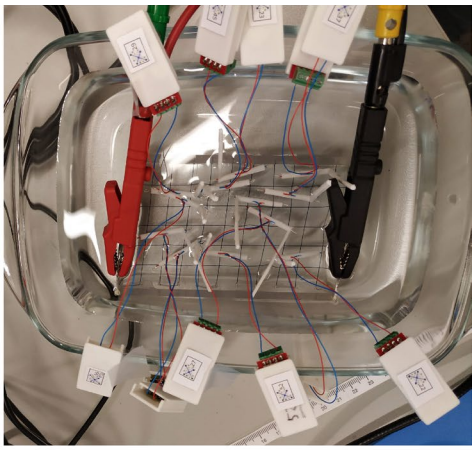

Fig. 3. Test bench. (a) Schematic representation of the setup used for the demonstration. Two aluminum external electrodes are held parallel and separated by two polycarbonate plates. This structure supports a cotton thread grid and is immersed into a glass container filled with saline. (b) Eleven miniature circuits are placed randomly between the two external electrodes.

and the external system knows the amount of information requested to the wireless devices, the algorithm detects the peaks and identifies if there are peaks lost in this first identification, knowing the approximate time difference between peaks. As the amplitudes of the peaks may differ significantly due to the power obtained by a specific device, the peak detection algorithm can analyze each uplink sequence independently of these amplitudes, improving the robustness of the decoding process with respect to the hardware-based system used in [7].

The last step was to decode the information by interpreting the peaks as '1's or '0's, performing a parity bit check, and running a Manchester decoder. The digital information obtained is then matched to the communication protocol to read the ACK message, the information related to the sensing or stimulation configuration, or the EMG sample obtained.

III. Results

The demonstration reported here was done using 11 different wireless devices, numbered in ascending order: 20, 21, 22, 23, 27, 29, 37, 45, 52, 154, 156. The devices were placed randomly between the two external electrodes, as shown in Fig. 3b. Their alignment with respect to the electric field delivered by the external system was also random, with a deviation of maximum 36º to ensure powering the devices with the WPT method proposed. Table 1 reports the final position of the electrodes for the x-y plane. The misalignment could be present in any of the three geometric planes.

The external system delivered HF current bursts with an amplitude of 50 V and 456 mA, with a frequency of 3 MHz, a burst duration of 1.6 ms and frequency of 50 Hz. These same bursts were used in [7]. All the devices were requested pings (i.e., replied with ACKs). Fig. 4 shows the waveforms obtained by the oscilloscope when IDs 21, 22 and 20 replied with ACKs. The devices were correctly addressed from the external system (downlink), and the uplink waveforms were successfully acquired by the oscilloscope regardless of the differences in amplitudes, as the oscilloscope´s trigger was synchronized from the external system.

TABLE I. Final x-y plane position of electrodes for demonstration

ID	Angle (º)	Center of electrode support	
		x-coordinate	y-coordinate
20	-36	2.8	1.5
21	-9	2.0	2.5
22	-16	9.0	1.5
23	-13	5.5	5.5
27	22	7.0	3.5
29	1	2.3	4.9
37	3	8.0	4.5
45	6	4.5	5.0
52	0	5.5	1.5
154	3	6.5	4.2
156	15	2.5	4.5

Fig. 5 shows the peak detection result for a ping requested to ID 37. The figure shows the least significant bit (LSB) and the most significant bit (MSB) of the frame, the peaks representing the bits and the predicted peaks that should have been identified knowing the timing between bits. The decoding algorithm was able to identify all the bits of the frame, perform parity bit check and Manchester decoding according to the communication protocol developed for the system.

IV. Discussion and Conclusions

Here we used a battery-powered oscilloscope to obtain the uplink waveforms, which were then digitally decoded offline. This oscilloscope could be replaced by a USB oscilloscope (e.g., PicoScope 5244D by Pico Technology) or a data acquisition board and a digital signal processor (DSP) to do the complete decoding process online, as it was the case of the hardware-based decoding system reported in [7]. However, the digital processing and decoding proposed here would be less susceptible to HF noise and the differences in modulation index generated by each implant. This could improve the robustness

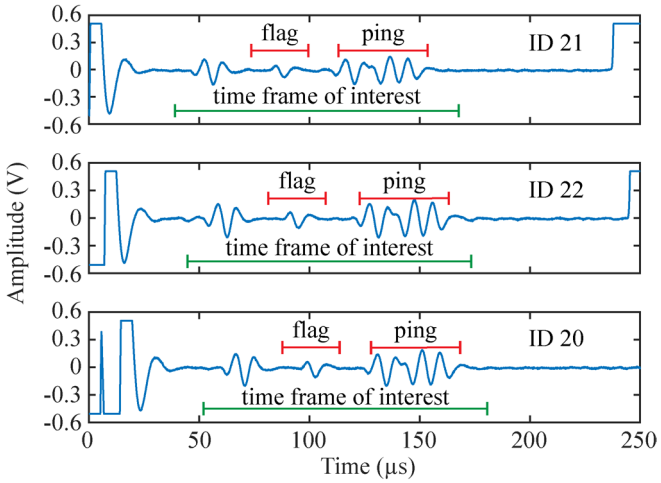

Fig. 4. Waveforms obtained using oscilloscope when external system requests a ping to three different wireless devices and the ACK is received from each circuit independently.

of the system and consolidate the closed-loop control for neuroprosthetic systems.

Some closed-loop neuroprosthetic systems require high data rates for real-time control, as that proposed in [1] for tremor reduction. To accomplish this, the communication protocol described in [7] allows to perform parametric acquisition (e.g., rms) to speed up the uplink sequences.

Communication by volume conduction is currently commercially used. For example, the MicroCam is a capsule endoscope that transmits images to an external system by means of volume conduction while the patient can do daily activities as walking [10], demonstrating that communication through volume conduction is not affected in common environments. However, not until recently it has been proposed the use of volume conduction both as a WPT and bidirectional communications method. In this combination, powering challenges prevail over those of communication. For instance, the power obtained by the devices depends on their alignment with respect to the electric field delivered by the external system. In [8] it was demonstrated that wireless devices could power with misalignments of up to 45º. This limitation appears earlier than those related to the communications between implants and their external system. We are currently working towards an

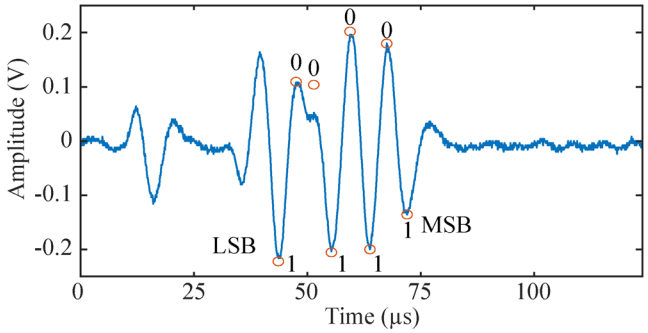

Fig. 5. Example of digital detection of bits for a short frame (ping ACK) made by ID 37. The value for ACK is obtained after Manchester decoding the value 169.

in-depth analysis of the powering and communications method to quantify the signal-to-noise ratio and bit error rate.

Implants powered by volume conduction require only electronic components that can be easily integrated in an application-specific integrated circuit (ASIC), accomplishing very thin and flexible microdevices. Even if the method requires applying large magnitude of HF current bursts to tissues to energize and communicate with the microdevices, it has been demonstrated that these bursts are innocuous and imperceptible if applied according to standards [11]. As illustrated here, WPT efficiency can be boosted when a large number of microdevices are powered and operated using the same energy used for a single device, offering an injectable microdevice technology of sensors and stimulators with high miniaturization capabilities for networked neural interphases.

ACKNOWLEDGMENT

This work has received funding from the European Research Council (ERC) - European Union's Horizon 2020 research and innovation programme under grant agreement No. 724244 (eAXON) and from the European Union's Horizon 2020 research and innovation programme under grant agreement No. 779982 (Project EXTEND - Bidirectional Hyper-Connected Neural System). AI gratefully acknowledges the financial support by ICREA under the ICREA Academia programme.

REFERENCES

[1] A. Pascual-Valdunciel *et al.*, "Intramuscular stimulation of muscle afferents attains prolonged tremor reduction in essential tremor patients," *IEEE Trans. Biomed. Eng.*, vol. 68, no. 6, pp. 1768–1776, 2020.

[2] F. Zurita *et al.*, "In vivo closed-loop control of a locust's leg using nerve stimulation," *Sci. Rep.*, vol. 12, no. 1, pp. 1–9, 2022.

[3] G. L. Barbruni, P. M. Ros, D. Demarchi, S. Carrara, and D. Ghezzi, "Miniaturised Wireless Power Transfer Systems for Neurostimulation: A Review," *IEEE Trans. Biomed. Circuits Syst.*, vol. 14, no. 6, pp. 1160–1178, 2020.

[4] K. Agarwal, R. Jegadeesan, Y.-X. Guo, and N. V. Thakor, "Wireless Power Transfer Strategies for Implantable Bioelectronics," *IEEE Rev. Biomed. Eng.*, vol. 10, pp. 136–161, 2017.

[5] A. Ivorra, "Remote Electrical Stimulation by Means of Implanted Rectifiers," *PLoS One*, vol. 6, no. 8, p. e23456, 2011.

[6] A. García-Moreno, A. Comerma-Montells, M. Tudela-Pi, J. Minguillon, L. Becerra-Fajardo, and A. Ivorra, "Wireless networks of injectable microelectronic stimulators based on rectification of volume conducted high frequency currents," *J. Neural Eng.*, vol. 19, no. 5, Jan. 2022.

[7] L. Becerra-Fajardo *et al.*, "Floating EMG Sensors and Stimulators Wirelessly Powered and Operated by Volume Conduction for Networked Neuroprosthetics," *J. Neuroeng. Rehabil.*, vol. 19, no. 57, 2022.

[8] L. Becerra-Fajardo, M. Schmidbauer, and A. Ivorra, "Demonstration of 2-mm-Thick Microcontrolled Injectable Stimulators Based on Rectification of High Frequency Current Bursts," *IEEE Trans. Neural Syst. Rehabil. Eng.*, vol. 25, no. 8, pp. 1343–1352, 2017.

[9] D. Andreuccetti, R. Fossi, and C. Petrucci, "An Internet resource for the calculation of the dielectric properties of body tissues in the frequency range 10 Hz - 100 GHz," *Website at http://niremf.ifac.cnr.it/tissprop/. IFAC-CNR, Florence (Italy), 1997. Based on data published by C.Gabriel et al. in 1996.*, 1997. .

[10] K.-N. Shim *et al.*, "Quality Indicators for Small Bowel Capsule Endoscopy," *Clin. Endosc.*, vol. 50, no. 2, pp. 148–160, Mar. 2017.

[11] J. Minguillon *et al.*, "Powering Electronic Implants by High Frequency Volume Conduction: In Human Validation," *IEEE Trans. Biomed. Eng.*, vol. 70, no. 2, pp. 659–670, 2023.